

University of Groningen

Photopharmacology

Velema, Wim

IMPORTANT NOTE: You are advised to consult the publisher's version (publisher's PDF) if you wish to cite from it. Please check the document version below.

Document Version

Publisher's PDF, also known as Version of record

Publication date:

2014

[Link to publication in University of Groningen/UMCG research database](#)

Citation for published version (APA):

Velema, W. (2014). *Photopharmacology*. [Thesis fully internal (DIV), University of Groningen]. University of Groningen.

Copyright

Other than for strictly personal use, it is not permitted to download or to forward/distribute the text or part of it without the consent of the author(s) and/or copyright holder(s), unless the work is under an open content license (like Creative Commons).

The publication may also be distributed here under the terms of Article 25fa of the Dutch Copyright Act, indicated by the "Taverne" license. More information can be found on the University of Groningen website: <https://www.rug.nl/library/open-access/self-archiving-pure/taverne-amendment>.

Take-down policy

If you believe that this document breaches copyright please contact us providing details, and we will remove access to the work immediately and investigate your claim.

Downloaded from the University of Groningen/UMCG research database (Pure): <http://www.rug.nl/research/portal>. For technical reasons the number of authors shown on this cover page is limited to 10 maximum.

Chapter 5

Proteasome Inhibitors with Photocontrolled Activity

Mickel J. Hansen¹, Willem A. Velema¹, Gerjan de Bruin², Herman S. Overkleeft², Wiktor Szymanski^{1,3} and Ben L. Feringa¹

Chembiochem 2014; 15: 2053

Proteasome inhibitors are widely used in cancer treatment as chemotherapeutic agents. However, their employment often results in severe side effects, due to their non-specific cytotoxicity towards healthy tissue. This problem might be overcome using a photopharmacological approach, i.e. attaining external, dynamic photocontrol with precision in time and space over the activity of a cytotoxic agent, realized by the introduction of a photoswitchable moiety into its molecular structure. Here, we describe the design, synthesis and activity of photoswitchable proteasome inhibitors. A significant difference in proteasome inhibitory activity in cell extracts was observed before and after irradiation with light. The results presented in this chapter show high potential for the development of chemotherapeutic agents that can be switched on and off with light and would be useful in cancer treatment, constituting a new strategy for spatiotemporal modulation of proteasomal activity.

¹Stratingh Institute for Chemistry, University of Groningen, Groningen, The Netherlands. ²Gorlaeus Laboratories, Leiden Institute of Chemistry, Leiden, The Netherlands. ³Department of Radiology, University of Groningen, University Medical Center Groningen, Groningen, The Netherlands.

N.B. The work described in this chapter was performed by M. J. Hansen as part of his Master's thesis, under the guidance of W. A. Velema.

5.1 Introduction

Cancer is often treated with a combination of surgery, radiation therapy and chemotherapy.¹ While, in many cases, chemotherapy has proven to cure cancer and alleviate symptoms, it is notorious for its often severe adverse effects. Such effects can be caused by poor selectivity of the chemotherapeutic agent, but also because the primary biological function, targeted by the drug, is essential to healthy tissue as well.² One option to overcome adverse side effects is by developing chemotherapeutic agents whose biological activity can be dynamically and externally controlled in space and time.³

Photopharmacology,^{4,5} a strategy that relies on the incorporation of a photoswitchable moiety into the molecular structure of a bioactive molecule,^{6,7} holds great promise for gaining spatiotemporal control over cancer drug activity. By irradiating with light, photoresponsive molecules can be switched between two isomeric states, which show a difference in biological activity. This method has been used, *inter alia*, for the photocontrol of antibiotic activity⁸ and pain perception.^{9,10}

Exploiting the photopharmacological approach, a chemotherapeutic agent can be envisaged that is switched between a state of high and low activity, using light. The advantages of such an approach are twofold: i) low activity can be warranted in healthy tissue, avoiding adverse effects; ii) a higher concentration of bioactive chemotherapeutic agent can be established at the site of the tumor, making the treatment more effective.

Proteasome inhibitors are promising chemotherapeutic agents and Bortezomib (Velcade, Figure 1A) is the first drug of this group that was clinically approved for the treatment of multiple myeloma and mantle cell lymphoma.^{11,12} Proteasome inhibitors block one or more of the catalytic sites of the proteasome, which is a complex of proteolytic enzymes responsible in cells for the degradation of redundant, ubiquitin-tagged proteins.^{13–15} The catalytic sites, which can be discriminated as bearing peptidyl-glutamyl peptide-hydrolyzing (PGPH)-like (β 1), trypsin-like (β 2) or chymotrypsin-like (β 5) activity, are located inside the tunnel-shaped structure of the 20S proteasome core particle. These catalytic sites and their immunoproteasome equivalents (up-regulated by stimuli like oxidative stress and pro-inflammatory cytokines¹⁶), are instrumental in the degradation of the majority of cytosolic and nuclear proteins, as well as misfolded proteins dislocated from the endoplasmic reticulum (ER) to the cytoplasm, in most cell types throughout the kingdoms of life. Inhibition of one or more of the proteasome active sites leads to accumulation of

redundant proteins and peptides inside the cell, which is particularly damaging to tumor tissue.^{17,18} In tumor tissue, protein biosynthesis rates are often largely enhanced, particularly also in the ER. As a result, a large portion of the newly synthesized ER proteins does not pass the quality control and become proteasome substrates. Blocking proteasomal functioning leads to accumulation of these proteins, which triggers – when the burden becomes too high – apoptosis. Since proteasomes are essential to healthy tissue, it is not surprising that proteasome inhibitors exhibit an adverse effect on healthy cells as well, resulting in frequent side-effects, such as peripheral neuropathy and gastro-intestinal complications.^{11,19–21}

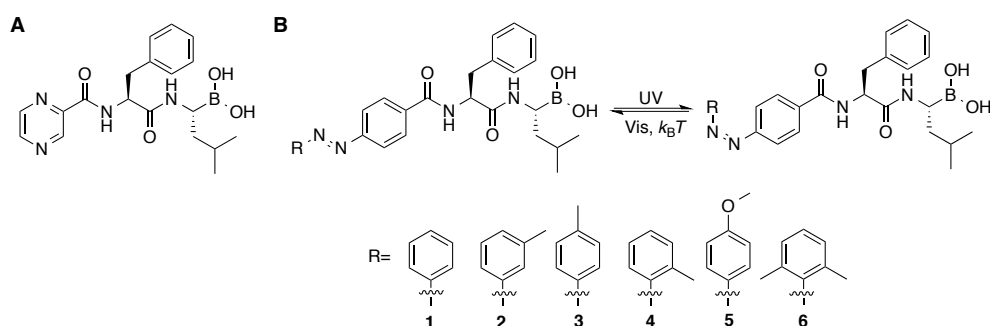


Figure 1 Molecular structures of bortezomib and photoswitchable proteasome inhibitors. A) Structure of bortezomib. B) Structures of photoswitchable proteasome inhibitors **1–6**. UV-irradiation switches the *trans*-isomer to the *cis*-isomer. Subsequent irradiation with visible light, or thermal relaxation, switches the *cis*-isomer back to the *trans*-isomer.

In this chapter, we describe the design, synthesis and inhibitory activity of photoswitchable proteasome inhibitors. Six different compounds (Figure 1) were prepared and their biological activity was assayed using competition experiments on cell lysates. A significant difference in proteasome inhibitory activity was found between the two photoisomeric forms of all compounds. The concept presented here with photoswitchable chemotherapeutic agents might be useful for more effective cancer treatment and reduction of side effects. Furthermore, the responsive inhibitors might be used as a tool in chemical biology studies to provide detailed insight into proteasome function.

5.2 Results and discussion

5.2.1 Design and synthesis of photoswitchable proteasome inhibitors

Bortezomib (Figure 1A) is a widely-used proteasome inhibitor.²² Its structure comprises a boronic acid 'warhead' that binds reversibly to the catalytic hydroxyl group in the active site of the proteasome, and a leucine-phenylalanine dipeptide that facilitates recognition and uptake by the proteasome (Figure 1A).²³ The leucine binds to the S1 pocket inside the 20S proteasome, whereas the phenylalanine binds to the S2 and the pyrazine moiety to the S3 pocket. Altogether, this peptide backbone forms an antiparallel beta-sheet through hydrogen bonding with the active sites. The major effect of bortezomib is observed on the $\beta 1/\beta 1i$ and $\beta 5/\beta 5i$ active sites whereas only little inhibition of the $\beta 2/\beta 2i$ active site is observed.¹³ Co-crystal structures of the proteasome-bound bortezomib reveal that the peptidic part of the bound bortezomib molecule fills a tight gap in the proteasome protein, as exemplified for the binding to the b5 binding site shown in Figure 2.^{24,25}

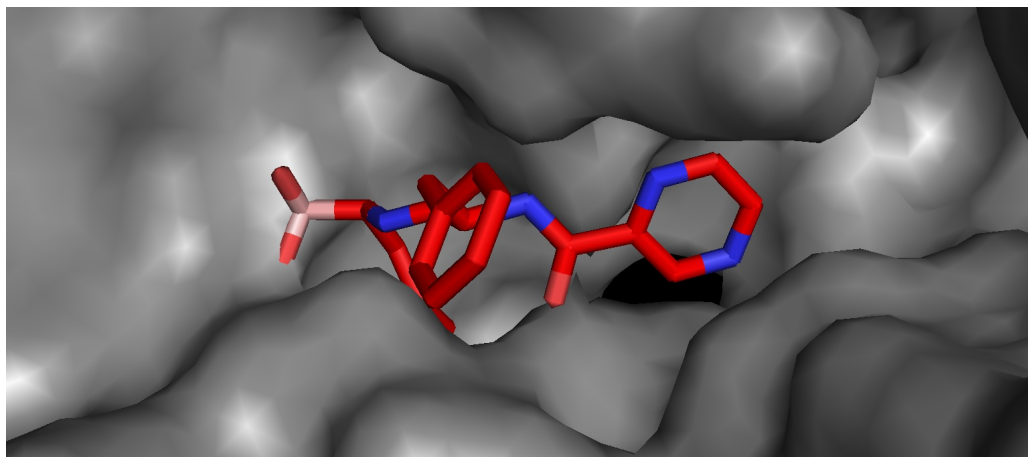


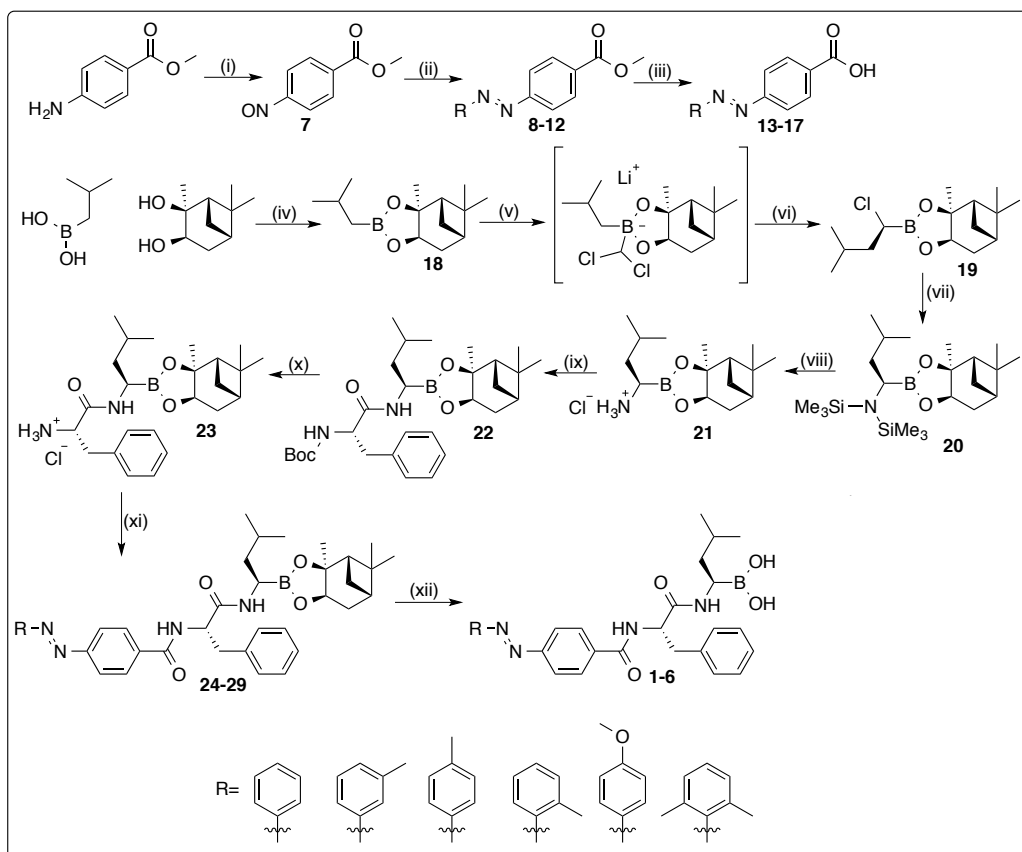
Figure 2 Co-crystal structure of bortezomib in complex with the 20S proteasome $\beta 5$ active site. (Groll et al.,²⁵ PDB: 2F16) The bortezomib structure fills a tight gap in the proteasome protein (grey).

Based on this data and SAR studies by Zhu et al.,²⁶ we envisioned that the attachment of an azobenzene photoswitch to the peptidic part of the bortezomib molecule could provide a bioactive compound with photocontrolled activity. More specifically, we expected the flat *trans* isomer of the compound to be able to fit in the tight gap in the active site. Upon photoisomerization to the *cis* form of the azobenzene, a large

conformational change, from planar to a non-planar structure, is observed.^{27–29} We envisioned that the large change in geometry and sterics caused by the non-planar *cis* conformation of the molecule would prevent its binding to the proteasome active sites. Based on these considerations, a series of six different, azobenzene-containing proteasome inhibitors were synthesized (compound **1-6**, Scheme 1).

Compounds **13-17** were prepared by sequential oxidation of methyl-4-aminobenzoate, a Mills reaction and saponification.

Compounds **1-6** were synthesized by sequential boronic ester formation from *isobutylboronic acid* and (+)-pinanediol, Matteson homologation, nucleophilic substitution reaction, TMS removal and amide formation with *N*-Boc-protected L-phenylalanine. Next, Boc deprotection and condensation with compounds **13-17** or 4-(phenyldiazenyl)-benzoic acid, and a final deprotection with *isobutylboronic acid*, afforded compounds **1-6**.

Scheme 1^a

^aReagents and conditions: (i) oxone, DCM, water (81%); (ii) AcOH, 40-70 °C, 15 h (59-95%); (iii) EtOH, 2.5 M aq. NaOH, 50 °C, 16 h (49-95%); (iv) Et₂O, rt, 24 h (>95%); (v) LDA, THF, DCM, -70 °C, 1 h; (vi) ZnCl₂/Et₂O, -78 °C, 1 h (81%); (vii) LiHMDS, THF, -78 °C - rt, 16 h (65%); (viii) 1.6 M HCl, dioxane/Et₂O (73%); (ix) Boc-Phe-OH, TBTU, DIPEA, DCM, -10 °C, 4 h (83%); (x) 0.89 M HCl, Et₂O, 0 °C, 16 h (94%); (xi) compound **13-17** or 4-(phenyldiazenyl)-benzoic acid, TBTU, DIPEA, DCM, -10 °C, 4 h (59-95%); (xii) Isobutyl boronic acid, MeOH, hexane, 1 M aq. HCl, rt, 17 h (35-77%).

5.2.2 Photochemical properties of photoswitchable proteasome inhibitors

Molecules that contain azobenzene moieties usually consist of mixtures of *trans* and *cis* isomers,³⁰⁻³⁴ with the *trans* isomer being the thermodynamically stable form. By irradiating the compounds with light of different wavelengths, the ratio between *trans* and *cis* isomers can be changed repetitively. Ideally, a large difference in ratio can be achieved, *i.e.*, switching between samples consisting of almost purely *trans* and almost purely *cis* isomer. Using UV-Vis spectroscopy and ¹H NMR spectroscopy, we

determined the *trans*:*cis* ratios (Table 1) and studied the photochemical isomerization of the photoswitchable proteasome inhibitors.

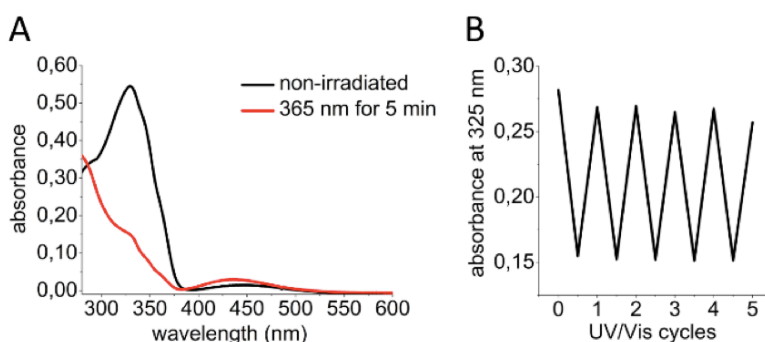


Figure 3 (A) UV–Vis absorption spectra of compound **1** in DMSO/H₂O (0.03 mM, <5 %_{vol} DMSO). (B) Reversible photochromism of compound **1** (20 mM) at pH = 7.4 in PBS (10 mM), GSH (10 mM) and DMSO (1%_{vol}).

The UV-Vis absorption spectra (see example in Figure 3) of compound **1-6** show an absorption maximum at ~340 nm, characteristic of *trans*-azobenzene.³⁰ After irradiation with $\lambda=365$ nm light, the absorption band decreases and a new absorption maximum appears at ~430 nm, distinctive of *cis*-azobenzene (Figure 3A).³⁰

Table 1 *Trans*:*cis* ratios of compounds **1-6** before and after irradiation ($\lambda_{irr}=365$ nm) (in DMSO-*d*₆/D₂O) and half-lives (in H₂O/DMSO(1%_{vol})) of the *cis*-isomers.

Compound	1	2	3	4	5	6
Non-irradiated (<i>trans</i> : <i>cis</i>)	97:3	89:11	93:7	91:9	97:3	65:35
Irradiated (<i>trans</i> : <i>cis</i>)	28:72	13:87	10:90	11:89	3:97	47:53
Half-life at 37 °C (hours)	6.8	7.7	5.4	6.6	3.8	5.8
λ_{max} (nm)	329	332	339	337	360	324

A major concern when incorporating azobenzene switches in biomolecules is their potential metabolic instability.⁴ This instability is caused by reduction of the azobenzene, either enzyme-mediated³⁵ or glutathione (GSH)-mediated,³⁶ towards hydrazobenzene. Concentrations up to 10 mM GSH can be found in the cytosol,³⁷ which makes GSH-mediated reduction a serious concern for the use of azobenzenes in bio-applications.⁴ To determine the stability of the photoswitchable proteasome

inhibitors against glutathione reduction,³⁸ reversible photochromism of compound **1** was determined in phosphate buffered saline (PBS) (10 mM, pH = 7.4) containing 10 mM GSH. As expected from earlier work by Woolley *et al.*,^{39,40} only little photo-bleaching was observed in the presence of GSH (Figure 3B), showing the applicability of incorporated azobenzene switches for cell studies.

Table 1 shows that the *trans*:*cis* ratios for compound **1-5** can be changed efficiently by irradiating the compounds at $\lambda=365$ nm. Compound **5** shows almost complete bidirectional switching (97:3 \leftrightarrow 3:97) between the pure *trans* and pure *cis* isomer, which has been observed before for 4-alkoxy-substituted azobenzenes.⁴¹ Compound **6** shows a smaller change in *trans*:*cis* ratio upon $\lambda=365$ nm light irradiation.

The half-life of the *cis*-form was determined by measuring the change in absorbance at the absorption maximum at 37° C in water (< 1%_{vol} DMSO) and was in the multi-hour range for all six compounds. This ensured only a minor change in *trans*:*cis* ratio during the competition assay (*vide infra*), which comprises a 90 min incubation step.

5.2.3 Biological activity of photoswitchable proteasome inhibitors

Competition experiments were performed on cell lysate, to study the biological activity of the photoswitchable proteasome inhibitors. For this purpose we performed an activity-based protein profiling assay, which relies on competition between the proteasome inhibitors and fluorescent, mechanism-based inhibitors, which specifically, covalently and irreversibly bind to one or more of the active sites of the proteasome.⁴²⁻⁴⁴ Cell lysates were incubated with increasing concentrations of compounds **1-6** for 1 h, after which the fluorescent probes were added and incubation continued for another 30 min. Subsequently, the cell lysates were loaded on a SDS gel. The fluorescence intensity of the bands on the gel can be related to the activity of the proteasome inhibitors, i.e., weak inhibitors will compete with the fluorescent probes only at high concentrations, whereas strong inhibitors will compete at lower concentrations (Figure 4). A clear difference in activity between the non-irradiated and the $\lambda=365$ nm light-irradiated compound **1** could be observed (Figure 4). The non-irradiated form, which contains 97% of *trans*-**1** (Table 1) is a stronger inhibitor of the b1i and b5 active sites, as compared to the $\lambda=365$ nm light-irradiated form, which contains 72% *cis*-**1** (Table 1). This is consistent with our hypothesis that the *trans*-form would be able to fit in the tight gap of the active site, whereas the conformation of the *cis*-form would hinder the binding.

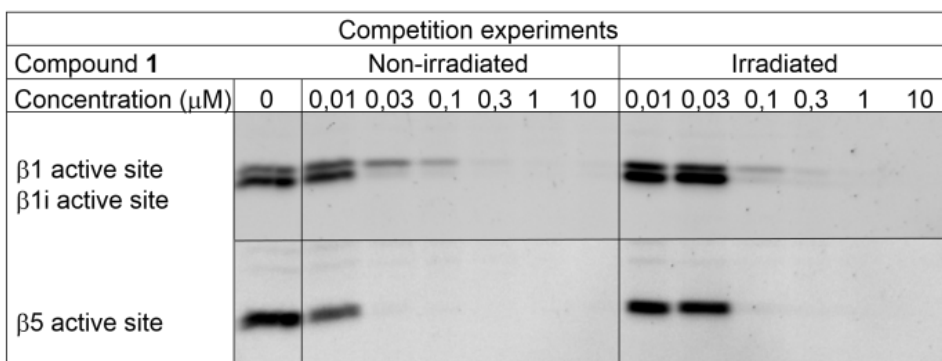


Figure 4 Results of fluorescence-based competition experiments for non-irradiated and irradiated compound **1**. IC_{50} values were obtained for all compounds for $\beta 1$, $\beta 1i$ and $\beta 5$ active sites before and after $\lambda=365$ nm irradiation. For non-irradiated compound **1**, disappearance of the fluorescent band is observed at 30 nM for the $\beta 1i$ and $\beta 5$ active site. After irradiation with $\lambda=365$ nm light, disappearance of these bands was observed at 100 nM.

To obtain quantitative data of the difference in activity between the non-irradiated and irradiated forms of compound **1-6**, IC_{50} values were determined (Table 2). By plotting the fluorescent intensity against inhibitor concentration, dose-response curves could be obtained and IC_{50} values were calculated (Table 2).

Table 2 IC_{50} values for compounds **1-6** for $\beta 1$, $\beta 1i$ and $\beta 5$ active sites before and after $\lambda=365$ nm light-irradiation, with all compounds showing a difference in activity on the $\beta 1$ active site, before and after $\lambda=365$ nm irradiation.

Active site	Compound	IC_{50} (nM)					
		1	2	3	4	5	6
$\beta 1$	Non-irradiated (<i>trans</i>)	29	41	25	26	46	70
	Irradiated (<i>cis</i>)	59	91	42	37	93	96
$\beta 1i$	Non-irradiated (<i>trans</i>)	14	16	16	16	16	16
	Irradiated (<i>cis</i>)	26	42	16	15	44	46
$\beta 5$	Non-irradiated (<i>trans</i>)	13	16	6	8	22	14
	Irradiated (<i>cis</i>)	23	22	9	10	32	11

Table 2 shows the active-site-specific difference in inhibitory activity between the non-irradiated and irradiated forms of compounds **1-6**. Depending on the substitution pattern of the aryldiazo group, a specific difference for the inhibition of the $\beta 1$, $\beta 1i$ or $\beta 5$ active sites could be observed. However, the general trend is that compounds that show a difference in activity on the $\beta 1$ active site, before and after irradiation, show a similar difference in activity on the $\beta 1i$ active site and a smaller difference is observed on the $\beta 5$ active site. Compound **1** (without substituents) shows a two-fold difference in activity between the non-irradiated and the irradiated form on all the active sites; compound **2** (*m*-methyl) shows an over two-fold difference in activity between non-irradiated and irradiated form for the $\beta 1$ active site whereas it shows an almost three-fold difference in activity for the $\beta 1i$ active site. However, compound **2** shows only a minor difference in activity between the isomers on the $\beta 5$ active site. This shows that a certain specificity can be obtained for the effect of *cis-trans* isomerization on one of the active sites. The same trend is observed for compound **5** (*p*-methoxy), which shows the largest difference in activity before and after irradiation for both $\beta 1$ (over two-fold) and $\beta 1i$ (almost three-fold) active sites whereas almost no difference is observed for the $\beta 5$ active site. Compounds **3** and **4**, with a methyl group at the *para*- and *ortho*-positions, respectively, show the smallest change in activity: still a significant difference in activity between non-irradiated and irradiated form for the $\beta 1$ active site was observed, whereas no or only minor differences were observed for the activity of both compounds towards the $\beta 1i$ and $\beta 5$ active sites. These results do not only demonstrate how, by modifying the substitution pattern on the aromatic ring, the change in activity between non-irradiated and irradiated forms can be increased, but also how the specificity for the effect on one of the active sites can be gained or lost. This constitutes a first step towards photoswitchable inhibitors with specificity for one of the active sites of the proteasome. By synthesizing and screening a small library of photoswitchable proteasome inhibitors, with various substituents it might become more clear which substitution pattern favors binding to a specific active site. This might be helpful information for designing compounds that are capable of changing the specificity from one active site to another, by photoisomerization.

To determine if a similar difference in inhibitory activity between non-irradiated and $\lambda=365$ nm light-irradiated forms could be observed on live cancerous cells, cytotoxicity assays were performed. Using a standard 3-(4,5-dimethylthiazol-2-yl)-2,5-diphenyltetrazolium bromide (MTT) assay,⁴⁵ the cytotoxicity of compounds **1-6** was determined on HeLa cells. Though a distinct difference in activity prior and after irradiation was observed for all compounds (For an example see Figure 5), the shape

of the dose-response curves changes as well. This indicates that other processes are at play that influence the cytotoxicity, before and after irradiation. One possibility might be that the more polar *cis*-form crosses the cell-membrane less efficiently, which causes the IC_{50} value to be higher and the shape of the dose-response curve to be different. In addition, the HeLa cells were incubated with the photoswitchable inhibitors for 16 hours. This is longer than the half-life of the *cis*-isomer of all compounds **1-6**. It means that significant amounts of the *cis*-form has been isomerized to the *trans*-form by thermal relaxation, which complicates the interpretation of the obtained data.

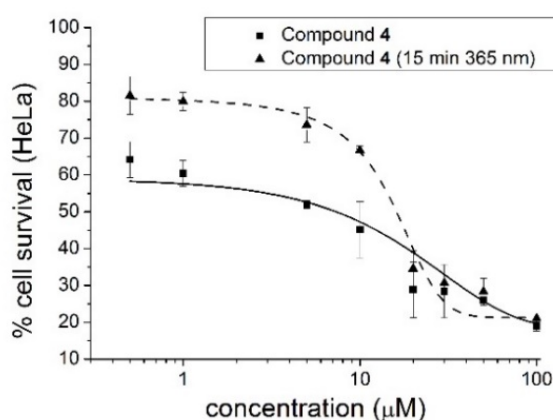


Figure 5 MTT assay for compound 4 in its non-irradiated (squares) and 365 nm-irradiated (triangles) forms.

5.3 Conclusion

In conclusion, we have successfully developed a set of proteasome inhibitors, whose activity could be altered by irradiation with light. The photoswitchable behavior of the compounds was characterized using UV-Vis spectroscopy and 1H NMR spectroscopy, giving information on *trans:cis* ratios and half-lives of the *cis*-isomer under the assay conditions. The change in inhibitory activity on the proteasome was determined using competition assays on cell lysate. A two- to three-fold change in activity on all three active sites, before and after exposure to $\lambda=365$ nm light, was observed, depending on the substitution pattern. The change in activity observed after *cis-trans* isomerization was further studied using cytotoxic MTT assays. These results provide the basis for the development of proteasome inhibitors whose activity

can be controlled with light, enabling dynamic control of cytotoxicity. Using this approach, a cytotoxic agent might be developed, that would be turned on and off inside the body. This could help to avoid severe side effects, by turning the chemotherapeutic agent off at the side of healthy tissue. Secondly, it might help the therapy to be more effective, because higher doses can be obtained at the site of the cancerous cells, without causing severe side-effects, which usually stem from high-dosing. In addition, the compounds might be used as a chemical biology tool to study the different active sites of the proteasome and might help to obtain more pharmacodynamic data of the mode of action of proteasome inhibitors.

Future research following this proof of concept should focus on the optimization of substitution patterns on the azobenzene switch to obtain a larger difference in activity and allow photo-isomerization with the more biocompatible red light, which is less toxic and allows deeper tissue penetration.^{39,46–48} Even though further optimization might be required for future applications, these results constitute a proof of principle for developing proteasome inhibitors, whose specificity towards one or more of the active sites might be changed using light.

5.4 Experimental section

5.4.1 Photoswitching Experiments

Irradiation experiments in H₂O/DMSO were performed with a Spectroline ENB-280C/FE UV lamp (365 nm) and Thor Labs OSL1-EC Fiber Illuminator (white light).

5.4.2 Competition Experiments

Lysates of RAJI cells (10 mg/9 ml) were prepared in 50 mM Tris pH 7.5, 5 mM MgCl₂, 2 mM ATP, 2 mM DTT and 10% glycerol. The cell lysates (9 µg total protein) were incubated with the different concentrations of the synthesized inhibitors (**1-6**) for 1 h at 37 °C in the dark. Next, the cell lysates were incubated with BODIPY-NC001 (Fig. S7) (1 mM) and BODIPY-NC005 (Fig. S7) (0,1 mM) for an additional 30 min at 37°C in the dark. This was followed by 5 min boiling with a reducing gel-loading buffer (4 ml) (20% SDS (1 ml), 0.6 M Tris HCl pH 6.8 (1 ml), 87% glycerol (2,1 ml), b-mercaptoethanol (0,4 ml), 10% BPB (0,1 ml), H₂O (MiliQ), and fractionation on 12.5% SDS-PAGE gel. In-gel detection of residual proteasome activity was performed in the wet gel slabs on a Typhoon Variable Mode Imager (Amersham Biosciences) using the Cy2 settings (to detect BODIPY-FL-Ala-Pro-Nle-Leu-EK, BODIPY-NC001) and Cy3 settings, to detect BODIPY-TMR-MeTyr-Phe-Leu-VS, BODIPY-NC005).⁴⁴ Intensities of

$\beta 1/\beta 1i$ and $\beta 5$ bands were measured by fluorescent densitometry and normalized to mock treated samples, and the values of three independent experiments were plotted. Average IC_{50} (inhibitor concentrations giving 50% inhibition) values and standard deviations were obtained from fitted dose response curves.

5.4.3 Cell Culture

HeLa cells were grown in Dulbecco's Modified Eagle's Medium (DMEM) supplemented with 10% fetal calf serum, penicillin (100 units/mL), streptomycin (100 μ g/mL) and L-glutamine (2 mM). Cells were cultured at 37 °C, 5% CO_2 and 95% relative humidity.

5.4.4 Cytotoxicity Assay

The cytotoxicity of the studied compounds were determined using a standard 3-(4,5-dimethylthiazol-2-yl)-2,5-diphenyltetrazolium bromide (MTT) assay.⁴⁵ In short, HeLa cells were dispensed in a sterile 96-well plate at a cell density of 10,000 cells/well and were incubated for 8 h at 37 °C, 5% CO_2 and 95% relative humidity. Next, the compounds were added to the cells at various concentrations and were incubated for 16 h. Then MTT was added to a final concentration of 0.5 mg/mL in each well, followed by incubation for 4 h. After this period, all medium was removed and 100 μ L of DMSO was added. The absorbance was measured at 570 nm using a microplate reader (SynergyMX, BioTek). Cell survival was expressed as a relative viability of cells compared to control cultures that were incubated with medium only.

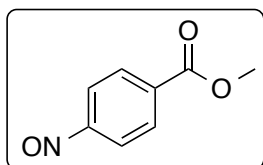
5.4.5 Synthesis

For general experimental information see section 2.5.6.

Methyl-4-nitrosobenzoate (7) A mixture of methyl-4-aminobenzoate (3.30 mmol, 500 mg) and oxone (6.60 mmol, 4.10 g) in DCM (10 mL) and H_2O (50 mL) was stirred at room temperature for 3 h. The organic layer was separated and the aqueous layer was extracted with DCM (2 x 20 mL), the combined organic layers were washed with 1M aqueous HCl (30 mL) and brine (20 mL) and dried ($MgSO_4$). Drying *in vacuo* and recrystallization from ethyl acetate resulted in 431 mg (79%) of a bright yellow solid. mp: 132-133 °C (lit. 123-125 °C).

1H NMR (400 MHz, $CDCl_3$): δ 8.30 (d, J = 8.6 Hz, 2H), 7.94 (d, J = 8.6 Hz, 2H), 3.98 (s, 3H). (in accordance to literature)

^{13}C NMR (100 MHz, $DMSO-d_6$): δ 165.7, 164.3, 135.1, 131.0, 120.3, 52.7.



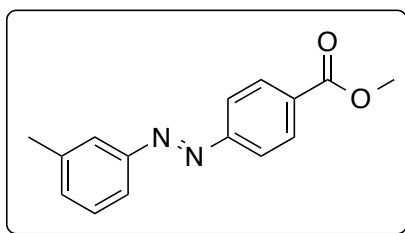
HR-MS (ESI, $[M+H]^+$): Calcd. for $C_8H_8NO_3$: 166.0499 ; Found: 166.0414

1H NMR spectrum in agreement with published data.⁴⁹

Compounds **8-12**

Compound **7** (1 eq) and an aniline (1.1 eq) were added to acetic acid (0.12 mmol/mL) and the mixture was stirred for 16 h at 40 °C. The solution was diluted with water, extracted with DCM, dried ($MgSO_4$) and the solvent evaporated *in vacuo*. If necessary, the product was purified by flash chromatography (silicagel, 40-63 μm , pentane/diethylether), the products were obtained as orange solids.

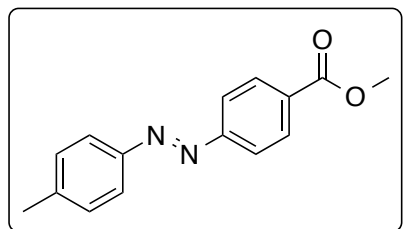
(E)-methyl 4-(m-tolyldiazenyl)benzoate (8) 101 mg (66%) of the product was obtained as deep orange crystals. mp: 104-105 °C.



1H NMR (400 MHz, $CDCl_3$): δ 8.19 (d, J = 8.4 Hz, 2H), 7.94 (d, J = 8.4 Hz, 2H), 7.76 (m, 2H), 7.43 (t, J = 7.9 Hz, 1H), 7.33 (d, J = 7.9 Hz, 1H), 3.96 (s, 3H), 2.47 (s, 3H).

^{13}C NMR (100 MHz, $CDCl_3$): δ 166.5, 155.2, 152.6, 139.1, 132.5, 131.7, 130.6, 130.2, 128.9, 125.3, 123.2, 122.6, 120.8, 52.3, 21.4.
HR-MS (ESI, $[M+H]^+$): Calcd. for $C_{15}H_{15}N_2O_2$: 255.1128 ; Found: 255.1124

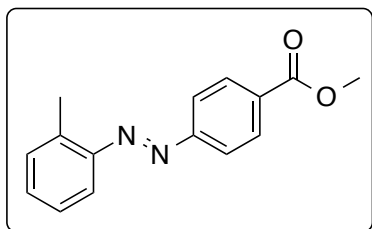
(E)-methyl 4-(p-tolyldiazenyl)benzoate (9) 150 mg (>95%) of the product was obtained as light orange crystals. mp: 138-139 °C.



1H NMR (400 MHz, $CDCl_3$): δ 8.22 (d, J = 8.4 Hz, 2H), 7.93 (d, J = 8.4 Hz, 2H), 7.86 (d, J = 8.4 Hz, 2H), 7.33 (d, J = 8.6 Hz, 2H), 3.96 (s, 3H), 2.45 (s, 3H).

^{13}C NMR (100 MHz, $CDCl_3$): δ 166.6, 155.2, 150.7, 142.4, 131.5, 130.6, 129.8, 123.2, 122.5, 52.3, 21.6.
HR-MS (ESI, $[M+H]^+$): Calcd. for $C_{15}H_{15}N_2O_2$: 255.1128 ; Found: 255.1124

(E)-methyl 4-(o-tolyldiazenyl)benzoate (10) 106 mg (69%) of the product was obtained as a deep orange solid. mp: 101-102 °C.

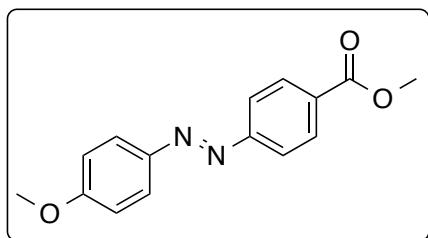


1H NMR (400 MHz, $CDCl_3$): δ 8.19 (d, J = 8.7 Hz, 2H), 7.98 (d, J = 8.6 Hz, 2H), 7.66 (d, J = 7.7 Hz, 1H), 7.43 – 7.34 (m, 2H), 7.29 (d, J = 8.2 Hz, 1H), 3.96 (s, 3H), 2.75 (s, 3H).

^{13}C NMR (100 MHz, $CDCl_3$): δ 166.6, 155.4, 150.6, 138.9, 131.7, 131.6, 131.4, 130.6, 126.4, 122.7, 115.3, 52.3, 17.5.

HR-MS (ESI, $[M+H]^+$): Calcd. for $C_{15}H_{15}N_2O_2$: 255.1128 ; Found: 255.1124

(E)-methyl 4-((4-methoxyphenyl)diazenyl)benzoate (11) 159 mg (>95%)



of the product was obtained as deep orange crystals. mp: 168-169 °C

1H NMR (400 MHz, $CDCl_3$): δ 8.17 (d, J = 8.6 Hz, 2H), 7.96 (d, J = 9.0 Hz, 2H), 7.91 (d, J = 8.6 Hz, 2H), 7.03 (d, J = 9.0 Hz, 2H), 3.96 (s, 3H), 3.91 (s, 3H).

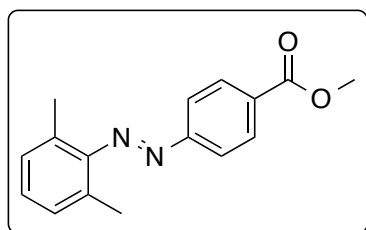
^{13}C NMR (100 MHz, $CDCl_3$): δ 166.6, 162.7, 155.3, 146.9, 131.2, 130.5, 125.2, 122.3, 114.3,

55.6, 52.3.

HR-MS (ESI, $[M+H]^+$): Calcd. for $C_{15}H_{14}N_2O_3$: 270.1004 ; Found: 270.1002

1H NMR spectrum in agreement with published data.⁵⁰

(E)-methyl 4-((2,6-dimethylphenyl)diazenyl)benzoate (12) 143 mg (59%)



of product was obtained as an orange solid. mp: 61-62 °C.

1H NMR (400 MHz, $DMSO-d_6$): δ 8.16 (d, J = 8.4 Hz, 2H), 7.94 (d, J = 8.5 Hz, 2H), 7.27 – 7.17 (m, 3H), 3.89 (s, 3H), 2.33 (s, 6H).

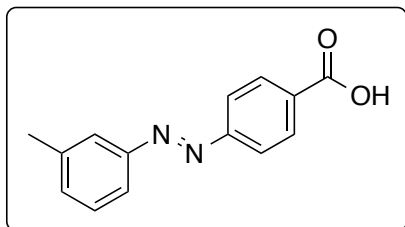
^{13}C NMR (100 MHz, $CDCl_3$): δ 166.4, 153.9, 149.2, 131.4, 130.6, 129.3, 128.9, 123.0, 122.3, 52.4, 19.2.

HR-MS (ESI, $[M+H]^+$): Calcd. for $C_{16}H_{17}N_2O_2$: 269.1285 ; Found: 269.1281

Compounds 13-17

Compound **8-12** (1 eq) was added to a solution of 2.5M aqueous NaOH (1 mmol/mL) in EtOH (0.04 mmol/mL) and the mixture was stirred at 50 °C for 16 h. Subsequently, 1M aqueous HCl was added and the mixture was extracted with DCM and after drying ($MgSO_4$) the solvent was evaporated *in vacuo*. If necessary, the product was purified by flash chromatography (silicagel, 40-63 μm , DCM/MeOH), the products were obtained as orange solids.

(E)-4-(m-tolyldiazenyl)benzoic acid (13) 47 mg (49%) of product was



obtained an orange solid. mp: 206-207 °C

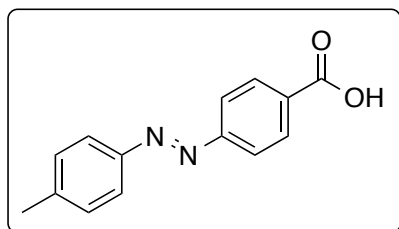
1H NMR (400 MHz, $CDCl_3$): δ 8.26 (d, J = 8.5 Hz, 2H), 7.98 (d, J = 8.6 Hz, 2H), 7.77 (m, 2H), 7.44 (t, J = 8.0 Hz, 1H), 7.34 (d, J = 7.6 Hz, 1H), 2.48 (s, 3H).

^{13}C NMR (100 MHz, $CDCl_3$): δ 170.4, 155.7, 152.6, 139.1, 132.6, 131.3, 130.6, 129.0, 123.3,

122.7, 120.8, 21.3.

HR-MS (ESI, $[M+H]^+$): Calcd. for $C_{14}H_{13}N_2O_2$: 241.0972 ; Found: 241.0968

(E)-4-(p-tolyldiazenyl)benzoic acid (14) 75 mg (78%) of product was obtained as an orange solid. mp: 279-280 °C.



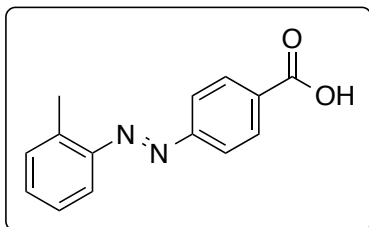
1H NMR (400 MHz, $DMSO-d_6$): δ 13.29 (s, 1H), 8.12 (d, J = 8.6 Hz, 2H), 7.93 (d, J = 8.7 Hz, 2H), 7.84 (d, J = 8.2 Hz, 2H), 7.42 (d, J = 8.6 Hz, 2H), 2.41 (s, 3H).

^{13}C NMR (100 MHz, $DMSO-d_6$): δ 167.1, 154.8, 150.5, 143.1, 133.0, 131.1, 130.5, 123.3, 122.9, 21.6.

HR-MS (ESI, $[M+H]^+$): Calcd. for $C_{14}H_{13}N_2O_2$: 241.0972 ; Found: 241.0968

1H NMR spectrum in agreement with published data.⁵¹

(E)-4-(o-tolyldiazenyl)benzoic acid (15) 95 mg (>95%) of product was obtained as an orange/red solid. mp: 231-232 °C.



1H NMR (400 MHz, $DMSO-d_6$): δ 13.24 (s, 1H), 8.13 (d, J = 8.4 Hz, 2H), 7.95 (d, J = 8.4 Hz, 2H), 7.59 (d, J = 8.3 Hz, 1H), 7.50 – 7.43 (m, 2H), 7.34 (t, J = 7.1 Hz, 1H), 2.69 (s, 3H).

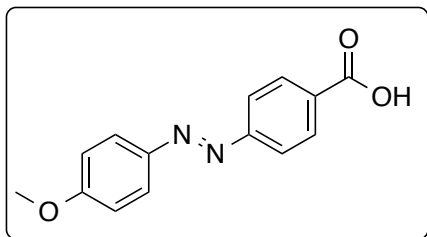
^{13}C NMR (100 MHz, $DMSO-d_6$): δ 167.2, 155.1, 150.4, 138.7, 133.2, 132.6, 132.0, 131.1, 127.2,

123.1, 115.5, 17.5.

HR-MS (ESI, $[M+H]^+$): Calcd. for $C_{14}H_{13}N_2O_2$: 241.0972 ; Found: 241.0969

1H NMR spectrum in agreement with published data.⁵¹

(E)-4-((4-methoxyphenyl)diazenyl)benzoic acid (16) 161 mg (>95%) of the product was obtained as an orange solid. mp: 249-251 °C.



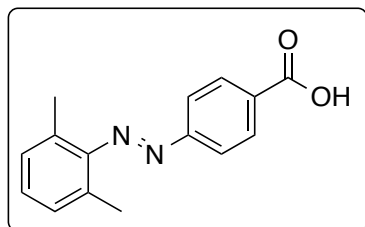
1H NMR (400 MHz, $DMSO-d_6$): δ 8.10 (d, J = 8.6 Hz, 2H), 7.93 (d, J = 9.0 Hz, 2H), 7.90 (d, J = 8.6 Hz, 2H), 7.15 (d, J = 9.1 Hz, 2H), 3.87 (s, 3H).

^{13}C NMR (100 MHz, $DMSO-d_6$): δ 167.2, 163.0, 154.9, 146.7, 132.6, 131.0, 125.5, 122.6, 115.2,

56.2.

HR-MS (ESI, $[M+H]^+$): Calcd. for $C_{14}H_{13}N_2O_3$: 257.0921 ; Found: 257.0918

1H NMR spectrum in agreement with published data.⁵²

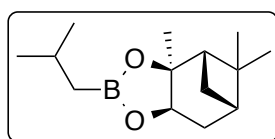
(E)-4-((2,6-dimethylphenyl)diazenyl)benzoic acid (17) 103 mg (84%) of

product was obtained as an orange solid. mp: 178–179 °C.

^1H NMR (400 MHz, $\text{DMSO}-d_6$): δ 13.20 (s, 1H), 8.14 (d, J = 8.2 Hz, 2H), 7.92 (d, J = 8.1 Hz, 2H), 7.23 (m, 3H), 2.32 (s, 6H).

^{13}C NMR (100 MHz, $\text{DMSO}-d_6$): δ 167.2, 155.0, 150.8, 133.3, 131.1, 129.7, 128.6, 122.6, 119.9, 19.1.

HR-MS (ESI, $[\text{M}+\text{H}]^+$): Calcd. for $\text{C}_{15}\text{H}_{15}\text{N}_2\text{O}_2$: 255.1128; Found: 255.1125

(S)-pinanediol (2-methylpropyl)boronate (18) A mixture of (+)-pinanediol

(7.0 mmol, 1.2 g) and isobutylboronic acid (7.0 mmol, 0.77 g) in Et_2O (9 mL) was stirred at room temperature for 24 h. Subsequently, the mixture was dried (MgSO_4) and the solvent was evaporated *in vacuo*. This resulted in 1.62 g (>95%) of a colorless oil.

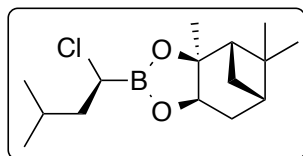
^1H NMR (400 MHz, $\text{DMSO}-d_6$): δ 4.27 (dd, J = 8.7, 1.9 Hz, 1H), 2.33 – 2.22 (m, 1H), 2.20 – 2.12 (m, 1H), 1.94 (t, J = 5.6 Hz, 1H), 1.88 – 1.80 (m, 1H), 1.76 (sext, J = 6.8 Hz, 1H), 1.71 – 1.62 (m, 1H), 1.28 (s, 3H), 1.23 (s, 3H), 0.99 (d, J = 10.6 Hz, 1H), 0.88 (d, J = 6.6 Hz, 6H), 0.80 (s, 3H), 0.67 (dd, J = 7.0, 1.9 Hz, 2H).

^{13}C NMR (100 MHz, $\text{DMSO}-d_6$): δ 85.2, 76.9, 51.2, 39.4, 38.2, 35.6, 28.9, 27.3, 26.5, 25.6, 25.5, 24.8, 24.1.

HR-MS (ESI, $[\text{M}+\text{H}]^+$): Calcd. for $\text{C}_{14}\text{H}_{26}\text{BO}_2$: 237.2020 ; Found: 237.2018

$[\alpha]_D^{20}$: 26.4 (c = 1.75, CHCl_3) (lit. 26.9 (c = 1.75, CHCl_3))⁵³

^1H NMR spectrum in agreement with published data.⁵⁴

(1S)-(S)-pinanediol 1-chloro-3-methylbutane-1-boronate (19) To a

solution of di-isopropylamine (0.35 mL) in dry THF (0.6 mL) at -50 °C a *n*-butyl lithium solution (2.5 mmol, 1.6 mL) in hexane was added dropwise, followed by warming up to -30 °C over 0.5 h. This solution was added over 0.5 h to a solution of **18** (2.10 mmol, 500 mg) in DCM (0.5 mL)

and dry THF (7.0 mL) at -70 °C. After 1 h a 1.0M ZnCl_2 (3.40 mmol, 462 mg) solution in Et_2O (3.4 mL) was added over 0.5 h at -78 °C and the reaction mixture was stirred under nitrogen for 3 hrs. Subsequently, the mixture was warmed up to room temperature, concentrated, and pentane (10 mL) was added together with 10% aqueous NH_4Cl solution. This mixture was extracted with pentane (2 x 3 mL) and dried (MgSO_4) and the solvent was evaporated *in vacuo*. This resulted in 484 mg (81%; 14% of **18**) of a pale yellow oil.

^1H NMR (400 MHz, $\text{DMSO}-d_6$): δ 4.43 (dd, J = 8.8, 1.6 Hz, 1H), 3.63 – 3.56 (m, 1H), 2.37 – 2.28 (m, 1H), 2.24 – 2.16 (m, 1H), 2.00 (t, J = 5.5 Hz, 1H), 1.91 – 1.84 (m, 1H),

1.79 – 1.72 (m, 2H), 1.71 – 1.56 (m, 2H), 1.34 (s, 3H), 1.26 (s, 3H), 1.08 (d, $J = 10.8$ Hz, 1H), 0.88 (dd, $J = 10.8, 6.5$ Hz, 6H), 0.82 (s, 3H).

^{13}C NMR (100 MHz, DMSO- d_6): δ 86.5, 77.8, 51.2, 42.8, 38.3, 35.3, 28.5, 27.2, 26.2, 25.7, 25.6, 24.0, 23.1, 22.2, 21.6.

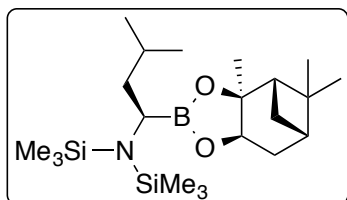
HR-MS (ESI, $[\text{M}+\text{H}]^+$): Calcd. for $\text{C}_{15}\text{H}_{26}\text{BClO}_2$: 284.1787 ; Found: 285.1784

$[\alpha]_{\text{D}}^{20}$: 27.0 ($c = 1.0$, MeOH)

^1H NMR spectrum in agreement with published data.⁵⁴

(1S)-(S)-pinanediol

boronate (20) A solution of 1M LiHMDS in THF (0.9 mL) was added over 0.5 h to a solution of **19** (0.870 mmol, 250 mg) in THF (3 mL) while cooling at -78°C . The mixture was stirred for 16 h and allowed to warm up to room temperature. The solvent was removed *in vacuo* and the residue was dissolved in hexane (8 mL) and stirred for 2 h at room temperature. Subsequently, the mixture was filtered through Celite® and washed with hexane. Drying *in vacuo* resulted in 231 mg (65%) of a colorless oil. The oil was used in subsequent steps without further purification



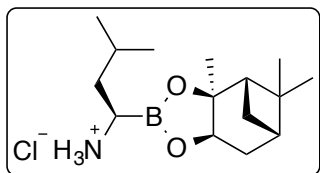
1-bis(trimethylsilyl)amino-3-methylbutane-1-

^1H NMR (400 MHz, DMSO- d_6): δ 4.34 (dd, $J = 8.7, 1.7$ Hz, 1H), 2.58 (dd, $J = 8.7, 6.7$ Hz, 1H), 2.34 – 2.24 (m, 1H), 2.22 – 2.13 (m, 1H), 1.95 (t, $J = 5.5$ Hz, 1H), 1.88 – 1.83 (m, 1H), 1.80 – 1.55 (m, 3H), 1.30 (d, $J = 6.3$ Hz, 3H), 1.19 – 1.13 (m, 1H), 1.01 (dd, $J = 10.7, 4.5$ Hz, 1H), 0.89 (d, $J = 6.6$ Hz, 3H), 0.85 (d, $J = 3.1$ Hz, 6H), 0.80 (s, 3H), 0.07 (s, 18H).

^1H NMR spectrum in agreement with published data.⁵⁴

(1S)-(S)-pinanediol 1-ammonium-3-methylbutane-1-boronate, HCl salt

(21) To a solution of **20** (0.83 mmol, 340 mg) in a mixture of dioxane (0.5 mL) and Et_2O (1 mL) at 0°C a 4M HCl solution in dioxane (1 mL) was added. The mixture was stirred at room temperature for 4 h and concentrated *in vacuo*. The residue was dissolved in hexane (2.5 mL) and 2M HCl in diethyl ether (0.25 mL) was added. The mixture was stirred for 1 h at 0°C , concentrated and dissolved in dry hexane (2 mL).



This suspension was stirred for 1 h and the precipitate was filtered off. Drying of the precipitate resulted in 161 mg (73%) of a white solid.

^1H NMR (400 MHz, DMSO- d_6): δ 7.83 (s, 3H), 4.43 (d, $J = 7.2$ Hz, 1H), 2.75 (t, $J = 7.6$ Hz, 1H), 2.38 – 2.26 (m, 1H), 2.18 (dt, $J = 10.7, 5.4$ Hz, 1H), 1.99 (t, $J = 5.5$ Hz, 1H), 1.87 (m, 1H), 1.80 – 1.62 (m, 2H), 1.55 – 1.39 (m, 2H), 1.35 (s, 3H), 1.24 (s, 3H), 1.10 (d, $J = 10.8$ Hz, 1H), 0.84 (d, $J = 7.1$ Hz, 6H), 0.81 (s, 3H).

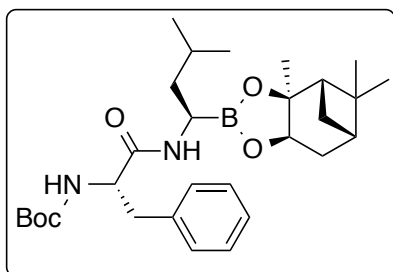
^{13}C NMR (100 MHz, DMSO-d_6): δ 87.1, 77.9, 51.1, 39.3, 38.7, 38.3, 35.1, 28.6, 27.3, 26.3, 24.7, 24.1, 22.7, 22.6.

HR-MS (ESI, $[\text{M}+\text{H}]^+$): Calcd. for $\text{C}_{15}\text{H}_{29}\text{BNO}_2$: 266.2286 ; Found: 266.2289

$[\alpha]_{\text{D}}^{20}$: 8.8 ($c = 1.0$, MeOH)

^1H NMR spectrum in agreement with published data.⁵⁴

(1S,2S,3R,5S)-Pinanediol N-BOC-L-phenylalanine-L-leucine boronate (22)



and TBTU (0.360 mmol, 117 mg) in DCM (1.1 mL) at $-5\text{ }^{\circ}\text{C}$ a solution of DIPEA (0.128 mL) in DCM (0.5 mL) was added during 2 h maintaining the temperature between -10 and $-5\text{ }^{\circ}\text{C}$. The mixture was stirred for another 1.5 h and slowly heated to room temperature. Subsequently, the solvent was removed *in vacuo* and the residue was dissolved in ethyl acetate (1.5 mL), washed with H_2O (1 mL), 3% KHCO_3 in H_2O (2.1 mL), H_2O (1 mL), 3%

aqueous citric acid (2.1 mL) and H_2O (1 mL). The solvent was removed *in vacuo* and the residue was dissolved in Et_2O and filtered through silica. Drying *in vacuo* resulted in 141 mg (83%) of a highly viscous oil.

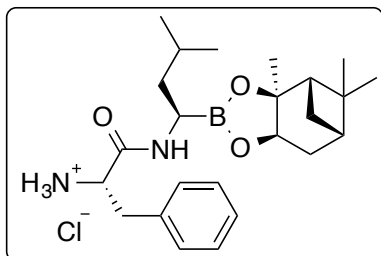
^1H NMR (400 MHz, DMSO-d_6): δ 8.85 (brs, 2H), 7.35 – 7.07 (m, 5H), 7.03 (d, $J = 8.3$ Hz, 1H), 4.28 – 4.18 (m, 1H), 4.08 (d, $J = 7.1$ Hz, 1H), 2.91 – 2.72 (m, 3H), 2.26 – 2.11 (m, 1H), 2.05 – 1.98 (m, 1H), 1.87 – 1.73 (m, 2H), 1.68 – 1.49 (m, 2H), 1.31 – 1.18 (m, 17H), 0.81 (s, 3H), 0.80 (s, 6H).

^{13}C NMR (100 MHz, DMSO-d_6): δ 174.8, 170.7, 155.5, 137.8, 129.6, 128.5, 128.4, 126.7, 83.2, 78.6, 76.1, 65.3, 60.1, 53.9, 52.2, 38.2, 29.4, 28.5, 27.6, 25.2, 24.4, 23.6, 22.4, 21.2, 15.6, 14.5.

HR-MS (ESI, $[\text{M}+\text{H}]^+$): Calcd. for $\text{C}_{29}\text{H}_{46}\text{BN}_2\text{O}_5$: 513.3494 ; Found: 513.3489

$[\alpha]_{\text{D}}^{20}$: -25.8 ($c = 1.0$, MeOH)

(1S,2S,3R,5S)-Pinanediol-L-phenylalanine-L-leucine boronate, HCl salt (23)



Compound **22** (0.08 mmol, 40 mg) was dissolved in Et_2O (2 mL) and 2M HCl in Et_2O (2.5 mL) was added keeping the temperature at $0\text{ }^{\circ}\text{C}$. The mixture was stirred for 16 h and allowed to slowly warm to room temperature. Filtration resulted in 32 mg (94%) of a bright yellow solid.

^1H NMR (400 MHz, DMSO-d_6): δ 8.62 (d, $J = 4.8$ Hz, 1H), 8.36 (s, 3H), 7.33 – 7.18 (m, 5H), 4.25 (dd, $J = 8.7$, 1.8 Hz, 1H), 4.00 (t, $J = 6.8$ Hz, 1H), 3.02 (d, $J =$

6.8 Hz, 2H), 2.89 – 2.78 (m, 1H), 2.33 – 2.20 (m, 1H), 2.14 – 2.05 (m, 1H), 1.92 (t, $J =$

5.5 Hz, 1H), 1.86 – 1.77 (m, 1H), 1.69 (d, $J = 14.2$ Hz, 1H), 1.58 – 1.34 (m, 1H), 1.30 (s, 3H), 1.23 (s, 3H), 1.31 – 1.12 (m, 3H), 0.86 – 0.69 (m, 9H).

^{13}C NMR (100 MHz, DMSO- d_6): δ 168.4, 135.3, 130.1, 128.7, 127.4, 85.3, 77.2, 53.0, 51.4, 40.2, 39.3, 38.2, 37.3, 35.6, 28.9, 27.4, 26.3, 24.9, 24.2, 23.4, 22.2.

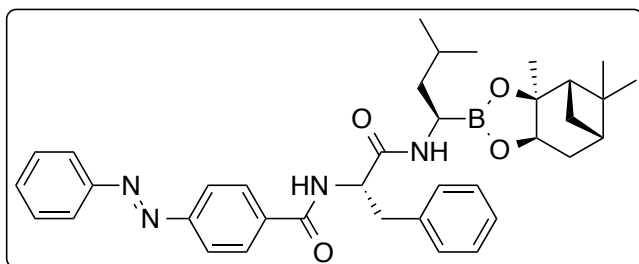
HR-MS (ESI, $[\text{M}+\text{H}]^+$): Calcd. for $\text{C}_{24}\text{H}_{38}\text{BN}_2\text{O}_3$: 413.2970 ; Found: 413.2973

$[\alpha]_{\text{D}}^{20}$: 7.4 ($c = 1.0$, MeOH)

Compounds **24-29**

To a solution of **23** (1 eq), **13-17** or 4-(phenyldiazenyl)-benzoic acid (1 eq) and TBTU (1.1 eq) in DCM (0.29 mmol/mL) at -5°C , a solution of DIPEA (2.2 eq) in DCM (1.3 mmol/mL) was added drop-wise over 2 h keeping the temperature at -10°C . The reaction mixture was stirred for another 1.5 h and slowly heated to room temperature. After evaporation *in vacuo* the residue was dissolved in EtOAc and washed with water, 3% aq. KHCO_3 solution, water, 3% aq. citric acid solution and water. The solution was dried (MgSO_4), concentrated and dissolved in Et_2O and filtered through silica. After evaporating the solvent *in vacuo*, products were obtained as an orange oil.

N-((R)-1-(((S)-3-methyl-1-((3aS,4S,6S,7aR)-3a,5,5-trimethylhexahydro-4,6-methanobenzo[d][1,3,2]dioxaborol-2-yl)butyl)amino)-1-oxo-3-phenylpropan-2-yl)-4-((E)-phenyldiazenyl)benzamide (24) 121 mg (>95%)



of product was obtained as an orange oil.

^1H NMR (400 MHz, DMSO- d_6): δ 8.95 (br s, 1H), 8.86 (d, $J = 8.2$ Hz, 1H), 7.98 (d, $J = 8.6$ Hz, 2H), 7.94 – 7.88 (m, 5H), 7.61 (d, $J = 6.5$ Hz, 2H), 7.33 (d, $J = 7.3$ Hz, 2H), 7.25

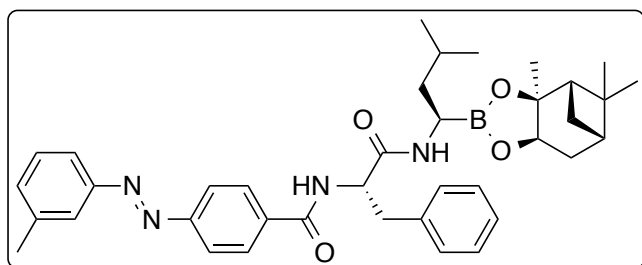
(t, $J = 7.5$ Hz, 2H), 7.16 (t, $J = 7.2$ Hz, 1H), 4.86 – 4.79 (m, 1H), 4.10 (dd, $J = 9.2$, 1.1 Hz, 1H), 3.05 (t, $J = 7.6$ Hz, 2H), 2.63 – 2.57 (m, 1H), 2.24 – 2.16 (m, 2H), 2.05 – 1.98 (m, 1H), 1.83 (t, $J = 5.6$ Hz, 1H), 1.80 – 1.74 (m, 1H), 1.66 – 1.57 (m, 2H), 1.30 (d, $J = 9.9$ Hz, 2H), 1.22 (d, $J = 13.6$ Hz, 6H), 0.82 (d, $J = 6.6$ Hz, 6H), 0.78 (s, 3H).

^{13}C NMR (100 MHz, DMSO- d_6): δ 173.9, 166.0, 153.8, 152.4, 138.1, 136.5, 132.4, 130.0, 129.6, 129.2, 128.5, 126.9, 123.2, 122.7, 120.4, 119.8, 83.5, 76.3, 53.3, 52.1, 38.1, 37.5, 36.5, 29.3, 27.6, 26.4, 25.3, 24.3, 23.5, 22.6.

HR-MS (ESI, $[\text{M}+\text{H}]^+$): Calcd. for $\text{C}_{37}\text{H}_{45}\text{BN}_4\text{O}_4$: 621.3607; Found: 621.3606

$[\alpha]_{\text{D}}^{20}$: -42.0 ($c = 0.5$, MeOH)

N-((R)-1-(((S)-3-methyl-1-((3a*S*,4*S*,6*S*,7a*R*)-3a,5,5-trimethylhexahydro-4,6-methanobenzo[d][1,3,2]dioxaborol-2-yl)butyl)amino)-1-oxo-3-phenylpropan-2-yl)-4-((E)-*m*-tolylidiazenyl)benzamide (25) 124 mg (59%)



of product was obtained as an orange oil.

^1H NMR (400 MHz, $\text{DMSO}-d_6$): δ 8.94 (d, J = 3.3 Hz, 1H), 8.85 (d, J = 8.4 Hz, 1H), 7.98 (d, J = 8.6 Hz, 2H), 7.90 (d, J = 8.6 Hz, 2H), 7.72 (d, J = 5.7 Hz, 2H), 7.49 (t, J = 7.9 Hz,

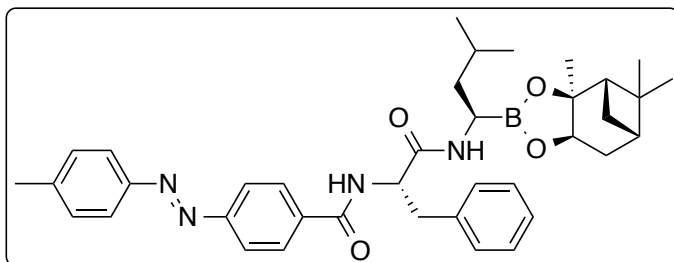
2H), 7.41 (d, J = 7.5 Hz, 1H), 7.33 (d, J = 7.2 Hz, 1H), 7.27 – 7.22 (m, 2H), 7.16 (t, J = 7.3 Hz, 1H), 4.86 – 4.79 (m, 1H), 4.11 (d, J = 6.8 Hz, 1H), 3.09 – 3.03 (m, 2H), 2.63 – 2.57 (m, 2H), 2.23 – 2.16 (m, 2H), 2.04 – 1.98 (m, 1H), 1.83 (t, J = 5.6 Hz, 1H), 1.80 – 1.75 (m, 1H), 1.66 – 1.57 (m, 2H), 1.33 – 1.25 (m, 4H), 1.23 (s, 3H), 1.20 (s, 3H), 0.82 (d, J = 6.6 Hz, 6H), 0.78 (s, 3H).

^{13}C NMR (100 MHz, $\text{DMSO}-d_6$): δ 173.9, 166.0, 153.8, 152.4, 139.5, 138.0, 133.1, 129.8, 129.6, 129.2, 128.5, 126.8, 126.6, 123.1, 122.6, 120.9, 83.5, 76.2, 53.2, 52.1, 40.1, 38.1, 37.5, 36.4, 29.3, 27.5, 27.2, 26.3, 25.2, 24.3, 23.4, 22.6, 21.3.

HR-MS (ESI, $[\text{M}+\text{H}]^+$): Calcd. for $\text{C}_{38}\text{H}_{48}\text{BN}_4\text{O}_4$: 635.3763; Found: 635.3755

$[\alpha]_D^{20}$: -36.4 (c = 1.0, MeOH)

N-((R)-1-(((S)-3-methyl-1-((3a*S*,4*S*,6*S*,7a*R*)-3a,5,5-trimethylhexahydro-4,6-methanobenzo[d][1,3,2]dioxaborol-2-yl)butyl)amino)-1-oxo-3-phenylpropan-2-yl)-4-((E)-*p*-tolylidiazenyl)benzamide (26) 136 mg (65%) of



product was obtained as a red/orange oil.

^1H NMR (400 MHz, $\text{DMSO}-d_6$): δ 8.94 (d, J = 3.1 Hz, 1H), 8.84 (d, J = 8.3 Hz, 1H), 7.97 (d, J = 8.6 Hz, 2H), 7.89 (d, J = 8.6 Hz, 2H), 7.82 (d, J = 8.3 Hz, 2H), 7.41 (d, J =

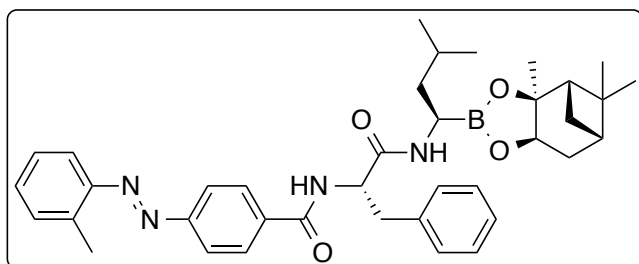
8.1 Hz, 2H), 7.33 (d, J = 7.2 Hz, 2H), 7.25 (t, J = 7.5 Hz, 2H), 7.16 (t, J = 6.8 Hz, 1H), 4.86 – 4.79 (m, 1H), 4.10 (d, J = 7.0 Hz, 1H), 3.10 – 3.00 (m, 2H), 2.63 – 2.57 (m, 1H), 2.40 (s, 3H), 2.23 – 2.17 (m, 1H), 2.05 – 1.97 (m, 1H), 1.83 (t, J = 5.5 Hz, 1H), 1.77 (s, 1H), 1.66 – 1.57 (m, 2H), 1.33 – 1.19 (m, 3H), 1.23 (s, 3H), 1.20 (s, 3H), 0.82 (d, J = 6.7 Hz, 6H), 0.78 (s, 3H).

^{13}C NMR (100 MHz, DMSO-d_6): δ 174.0, 166.0, 153.8, 150.5, 142.9, 138.0, 136.2, 130.5, 129.6, 129.2, 128.6, 126.8, 123.2, 122.5, 83.4, 76.2, 53.2, 52.0, 40.3, 39.7, 38.1, 37.5, 36.5, 29.3, 27.5, 26.3, 25.2, 24.3, 23.4, 22.6, 21.5.

HR-MS (ESI, $[\text{M}+\text{H}]^+$): Calcd. for $\text{C}_{38}\text{H}_{48}\text{BN}_4\text{O}_4$: 635.3763; Found: 635.3755

$[\alpha]_{\text{D}}^{20}$: -32.0 ($c = 1.0$, MeOH)

N-((R)-1-(((S)-3-methyl-1-((3aS,4S,6S,7aR)-3a,5,5-trimethylhexahydro-4,6-methanobenzo[d][1,3,2]dioxaborol-2-yl)butyl)amino)-1-oxo-3-phenylpropan-2-yl)-4-((E)-o-tolyldiazenyl)benzamide (27) 103 mg (>95%)



of product was obtained as a red/orange oil.

^1H NMR (400 MHz, DMSO-d_6): δ 8.94 (d, $J = 3.3$ Hz, 1H), 8.84 (d, $J = 8.4$ Hz, 1H), 7.99 – 7.96 (m, 2H), 7.92 – 7.89 (m, 2H), 7.57 (d, $J = 7.8$ Hz, 2H), 7.46 (dd, $J = 6.6, 0.8$ Hz,

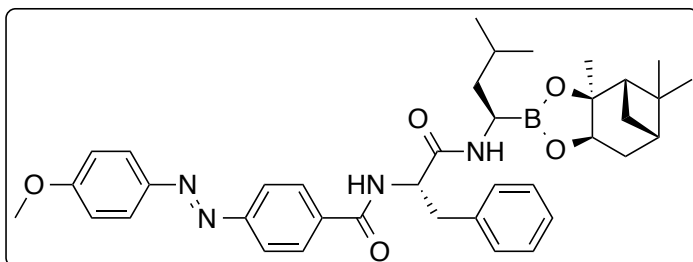
2H), 7.33 (d, $J = 6.9$ Hz, 3H), 7.25 (t, $J = 6.3$ Hz, 2H), 7.16 (t, $J = 6.1$ Hz, 1H), 4.86 – 4.79 (m, 1H), 4.11 (dd, $J = 8.5, 1.8$ Hz, 1H), 3.10 – 2.99 (m, 2H), 2.68 (s, 3H), 2.63 – 2.58 (m, 1H), 2.23 – 2.17 (m, 1H), 2.05 – 1.99 (m, 1H), 1.85 – 1.81 (m, 1H), 1.78 (dd, $J = 4.7, 3.2$ Hz, 1H), 1.66 – 1.57 (m, 2H), 1.34 – 1.24 (m, 2H), 1.24 (s, 3H), 1.20 (s, 3H), 0.83 (d, $J = 6.6$ Hz, 6H), 0.79 (s, 3H).

^{13}C NMR (100 MHz, DMSO-d_6): δ 175.8, 170.7, 150.3, 132.0, 129.6, 129.2, 128.6, 127.1, 122.7, 119.5, 115.5, 65.6, 60.2, 49.3, 48.2, 38.1, 35.5, 31.7, 30.2, 29.4, 29.2, 27.5, 25.6, 24.3, 23.4, 22.6, 22.5, 21.2, 19.1, 17.5, 14.5, 14.4, 11.7.

HR-MS (ESI, $[\text{M}+\text{H}]^+$): Calcd. for $\text{C}_{38}\text{H}_{48}\text{BN}_4\text{O}_4$: 635.3763; Found: 635.3754

$[\alpha]_{\text{D}}^{20}$: -34.8 ($c = 0.5$, MeOH)

4-((E)-(4-methoxyphenyl)diazenyl)-N-((R)-1-(((S)-3-methyl-1-((3aS,4S,6S,7aR)-3a,5,5-trimethylhexahydro-4,6-methanobenzo[d][1,3,2]dioxaborol-2-yl)butyl)amino)-1-oxo-3-phenylpropan-2-yl)benzamide (28) 163 mg (76%) of product was obtained as a red oil.



^1H NMR (400 MHz, DMSO-d_6): δ 8.94 (d, $J = 2.9$ Hz, 1H), 8.82 (d, $J = 8.4$ Hz, 1H), 7.96 (d, $J = 8.6$ Hz, 2H), 7.91 (d, $J = 9.0$ Hz, 2H), 7.86 (d, $J = 8.6$ Hz, 2H), 7.33 (d, $J = 7.1$ Hz, 2H), 7.25 (t, $J =$

7.5 Hz, 2H), 7.18 – 7.12 (m, 3H), 4.86 – 4.78 (m, 1H), 4.10 (dd, $J = 8.7, 2.0$ Hz, 1H),

3.86 (s, 3H), 3.10 – 3.01 (m, 2H), 2.63 – 2.56 (m, 1H), 2.24 – 2.15 (m, 1H), 2.06 – 1.97 (m, 1H), 1.83 (t, $J = 5.6$ Hz, 1H), 1.80 – 1.75 (m, 1H), 1.66 – 1.58 (m, 2H), 1.33 – 1.19 (m, 3H), 1.23 (s, 3H), 1.20 (s, 3H), 0.82 (d, $J = 6.6$ Hz, 6H), 0.79 (s, 3H).

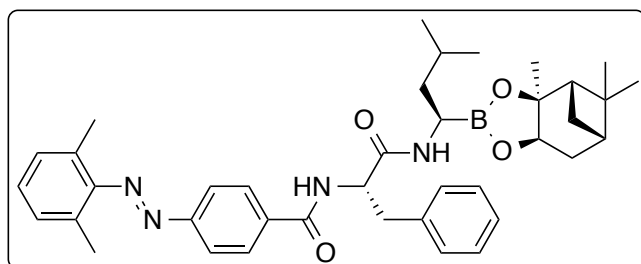
^{13}C NMR (100 MHz, DMSO- d_6): δ 174.1, 166.1, 162.9, 153.9, 146.7, 138.1, 135.8, 129.6, 129.2, 128.6, 126.8, 125.3, 123.8, 122.4, 119.3, 115.2, 114.3, 83.5, 76.3, 56.2, 53.2, 52.1, 38.1, 36.5, 29.3, 27.6, 26.4, 25.2, 24.4, 23.5, 22.6.

HR-MS (ESI, $[\text{M}+\text{H}]^+$): Calcd. for $\text{C}_{38}\text{H}_{48}\text{BN}_4\text{O}_5$: 651.3712; Found: 651.3707

$[\alpha]_D^{20}$: -38.6 ($c = 1.0$, MeOH)

4-((E)-(2,6-dimethylphenyl)diazenyl)-N-((R)-1-(((S)-3-methyl-1-((3aS,4S,6S,7aR)-3a,5,5-trimethylhexahydro-4,6-methanobenzo[d][1,3,2]dioxaborol-2-yl)butyl)amino)-1-oxo-3-phenylpropan-2-yl)benzamide (29) 161 mg (75%) of product was obtained as

an orange oil.



^1H NMR (400 MHz, DMSO- d_6): δ 8.94 (d, $J = 3.3$ Hz, 1H), 8.84 (d, $J = 8.4$ Hz, 1H), 7.98 (d, $J = 8.6$ Hz, 2H), 7.88 (d, $J = 8.6$ Hz, 2H), 7.33 (d, $J = 7.2$ Hz, 2H), 7.25 – 7.16 (m, 6H), 4.87 – 4.80 (m, 1H), 4.11 (dd,

$J = 8.7$, 1.9 Hz, 1H), 3.10 – 3.02 (m, 2H), 2.63 – 2.58 (m, 1H), 2.31 (s, 6H), 2.23 – 2.17 (m, 1H), 2.05 – 1.99 (m, 1H), 1.84 – 1.76 (m, 2H), 1.63 (m, 2H), 1.32 – 1.25 (m, 3H), 1.24 (s, 3H), 1.20 (s, 3H), 0.83 (d, $J = 6.6$ Hz, 6H), 0.79 (s, 3H).

^{13}C NMR (100MHz, DMSO- d_6): δ 174.1, 165.9, 154.1, 150.8, 138.0, 136.4, 131.0, 129.6, 129.6, 129.2, 128.6, 128.5, 127.3, 126.8, 122.3, 122.3, 119.7, 83.4, 76.3, 52.1, 38.1, 30.2, 29.3, 27.5, 25.3, 24.4, 23.5, 22.6, 19.1, 17.9, 17.9.

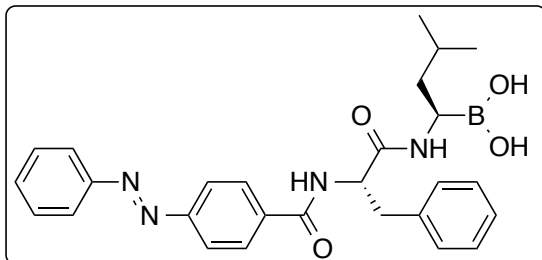
HR-MS (ESI, $[\text{M}+\text{H}]^+$): Calcd. for $\text{C}_{39}\text{H}_{50}\text{BN}_4\text{O}_4$: 649.3920; Found: 649.3912

$[\alpha]_D^{20}$: -37.2 ($c = 0.5$, MeOH)

Compounds **1-6**

To a stirred solution of **24-29** (1 eq) in MeOH (7.5 mL/mmol), hexane (7.5 mL/mmol) was added, followed by a solution of 1M aqueous HCl (1 mL/mmol). The reaction mixture was cooled to 10 °C. Isobutylboronic acid (2 eq) was added and the mixture was stirred for 17 h at room temperature. Subsequently, the layers were separated and the aqueous methanol layer was washed 3 times with hexane. The aqueous methanol layer was neutralized with aq. NaHCO_3 and extracted with EtOAc. The volatiles were evaporated *in vacuo* and the product was purified by flash chromatography (silicagel, 40-63 μm , DCM/Methanol, 9:1, v/v) resulting in an orange solid.

((S)-3-methyl-1-((R)-3-phenyl-2-(4-((E)-phenyldiazenyl)benzamido)butyl)boronic acid (1)



43 mg (56%) of product was obtained as an orange solid. mp: 133-134 °C.

^1H NMR (400 MHz, DMSO- d_6): δ 8.85 (d, J = 8.1 Hz, 1H), 8.80 (d, J = 8.2 Hz, 1H), 7.95 – 7.86 (m, 5H), 7.63 – 7.54 (m, 4H), 7.30 (d, J = 7.2 Hz, 2H), 7.23 (t, J = 7.5 Hz, 2H), 7.14 (t, J = 7.4 Hz, 1H), 4.67 (dd, J = 10.5, 4.4

Hz, 1H), 3.15 – 3.02 (m, 2H), 2.95 (dd, J = 13.6, 10.5 Hz, 1H), 1.56 – 1.45 (m, 1H), 1.38 – 1.24 (m, 2H), 0.80 (d, J = 7.0 Hz, 3H), 0.79 (d, J = 6.9 Hz, 3H).

^{13}C NMR (100 MHz, DMSO- d_6): δ 171.1, 166.2, 153.8, 152.3, 138.6, 136.4, 132.6, 130.1, 129.5, 129.1, 128.6, 126.8, 123.2, 122.8, 120.4, 119.9, 55.2, 25.3, 23.6, 22.4.

HR-MS (ESI, $[\text{M}+\text{Na}]^+$): Calcd. For $\text{C}_{27}\text{H}_{31}\text{BN}_4\text{O}_4\text{Na}$: 509.2336; Found: 509.2338

$[\alpha]_D^{20}$: -54.4 (c = 0.25, DMSO/ H_2O)

((S)-3-methyl-1-((R)-3-phenyl-2-(4-((E)m-tolyldiazenyl)benzamido)propanamido)butyl)boronic acid (2)

48 mg (61%) of product was obtained as an orange solid. mp: 102-103 °C.

^1H NMR (400 MHz, DMSO- d_6): δ 8.68 (d, J = 8.4 Hz, 1H), 7.95 – 7.86 (m, 5H), 7.63 – 7.54 (m, 4H), 7.30 (d, J = 7.2 Hz, 2H), 7.23 (t, J = 7.5 Hz, 2H), 7.14 (t, J = 7.4 Hz, 1H), 4.67 (dd, J = 10.5, 4.4 Hz, 1H), 3.15 – 3.02 (m, 2H), 2.95 (dd, J = 13.6, 10.5 Hz, 1H), 2.38

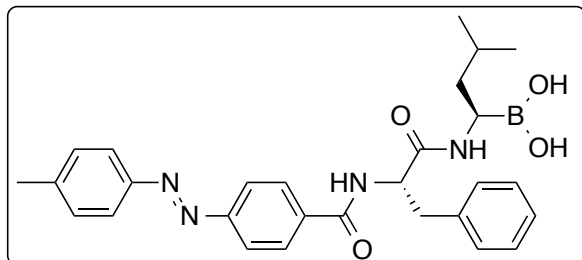
(s, 3H), 1.56 – 1.45 (m, 1H), 1.38 – 1.24 (m, 2H), 0.81 (d, J = 7.1 Hz, 3H), 0.79 (d, J = 6.9 Hz, 3H).

^{13}C NMR (100 MHz, DMSO- d_6): δ 171.2, 166.3, 153.8, 152.4, 139.7, 138.5, 136.3, 133.2, 129.9, 129.5, 129.1, 128.6, 126.8, 123.1, 122.7, 120.8, 55.2, 48.9, 31.6, 25.3, 23.6, 22.4, 21.2.

HR-MS (ESI, $[\text{M}+\text{Na}]^+$): Calcd. For $\text{C}_{28}\text{H}_{33}\text{BN}_4\text{O}_4\text{Na}$: 523.2487; Found: 523.2485

$[\alpha]_D^{20}$: 28.8 (c = 0.25, DMSO/ H_2O)

((S)-3-methyl-1-((R)-3-phenyl-2-(4-((E)-p-tolyldiazenyl)benzamido)propanamido)butyl)boronic acid (3)



28 mg (35%) of product was obtained as an orange solid. mp: 152-153 °C.

^1H NMR (400 MHz, $\text{DMSO}-d_6$): δ 8.64 (d, J = 8.4 Hz, 1H), 7.91 – 7.82 (m, 4H), 7.79 (d, J = 8.2 Hz, 2H), 7.38 (d, J = 8.2 Hz, 2H), 7.29 (d, J = 7.2 Hz, 2H), 7.23 (d, J = 7.2 Hz, 2H), 7.18 – 7.10 (m, 1H), 4.66 (dd, J = 10.4, 4.6 Hz, 1H),

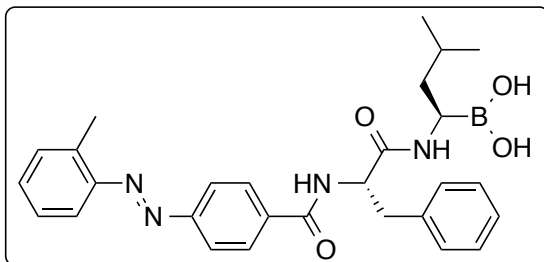
3.14 – 3.07 (m, 1H), 3.03 (m, 1H), 2.97 – 2.90 (m, 1H), 2.36 (s, 3H), 1.77 – 1.68 (m, 1H), 1.53 – 1.45 (m, 1H), 1.38 – 1.25 (m, 2H), 0.80 (d, J = 6.6 Hz, 3H), 0.78 (d, J = 6.6 Hz, 3H).

^{13}C NMR (100 MHz, $\text{DMSO}-d_6$): δ 171.3, 166.4, 153.9, 150.4, 143.2, 138.4, 136.1, 130.6, 129.5, 129.0, 128.6, 126.8, 123.4, 123.2, 122.6, 55.2, 37.4, 25.3, 23.6, 22.4, 21.5.

HR-MS (ESI, $[\text{M}+\text{Na}]^+$): Calcd. For $\text{C}_{28}\text{H}_{33}\text{BN}_4\text{O}_4\text{Na}$: 523.2487; Found: 523.2483

$[\alpha]_D^{20}$: -62.4 (c = 0.25, $\text{DMSO}/\text{H}_2\text{O}$)

((S)-3-methyl-1-((R)-3-phenyl-2-(4-((E)-o-tolyldiazenyl)benzamido)propanamido)butyl)boronic acid (4)



35 mg (44%) of product was obtained as an orange solid. mp: 123-127 °C

^1H NMR (400 MHz, $\text{DMSO}-d_6$): δ 8.69 (d, J = 8.4 Hz, 2H), 7.94 – 7.84 (m, 4H), 7.54 (d, J = 7.9 Hz, 1H), 7.47 – 7.40 (m, 2H), 7.35 – 7.31 (m, 1H), 7.30 (d, J = 7.0 Hz, 2H), 7.23 (d, J = 7.4 Hz, 2H), 7.14 (t, J = 7.3 Hz, 1H), 4.66 (dd, J = 10.5, 4.4 Hz, 1H), 3.11

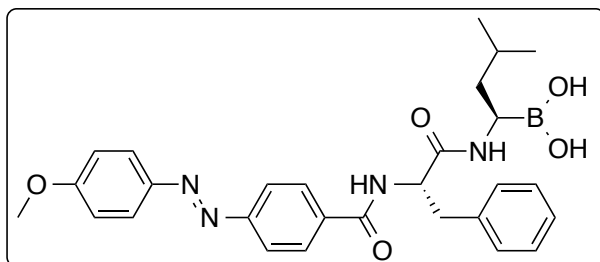
(dd, J = 13.8, 4.3 Hz, 1H), 3.04 (dd, J = 9.3, 5.7 Hz, 1H), 2.97 – 2.90 (m, 1H), 2.64 (s, 3H), 1.54 – 1.45 (m, 1H), 1.36 – 1.26 (m, 2H), 0.80 (d, J = 6.7 Hz, 3H), 0.78 (d, J = 6.7 Hz, 3H).

^{13}C NMR (100 MHz, $\text{DMSO}-d_6$): δ 171.2, 166.3, 154.2, 150.3, 138.6, 138.5, 136.2, 132.5, 132.0, 129.5, 129.0, 128.6, 127.2, 126.8, 122.8, 119.6, 115.5, 55.2, 37.4, 25.3, 23.6, 22.4, 17.5.

HR-MS (ESI, $[\text{M}+\text{Na}]^+$): Calcd. For $\text{C}_{28}\text{H}_{33}\text{BN}_4\text{O}_4\text{Na}$: 523.2487; Found: 523.2485

$[\alpha]_D^{20}$: -56.0 (c = 0.25, $\text{DMSO}/\text{H}_2\text{O}$)

((S)-1-((R)-2-(4-((E)-(4-methoxyphenyl)diazenyl)benzamido)-3-phenylpropanamido)-3-methylbutyl)boronic acid (5)



90 mg (77%) of product was obtained as an orange solid. mp: 250-255 °C (dec).

^1H NMR (400 MHz, DMSO- d_6): δ 8.69 (d, J = 8.6 Hz, 2H), 7.96 – 7.87 (m, 4H), 7.84 (d, J = 8.6 Hz, 2H), 7.32 (d, J = 7.3 Hz, 2H), 7.23 (t, J = 7.5 Hz, 2H), 7.17 – 7.09 (m, 3H), 4.67 (dd, J = 10.5,

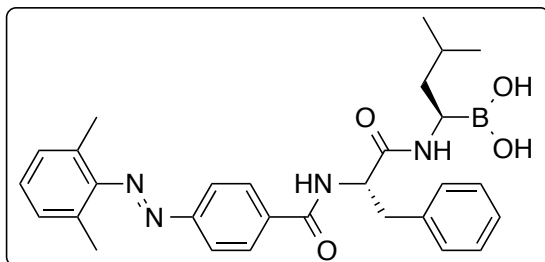
4.3 Hz, 1H), 3.85 (s, 3H), 3.11 – 3.05 (m, 2H), 3.00 – 2.93 (m, 1H), 1.58 – 1.49 (m, 1H), 1.37 – 1.27 (m, 2H), 0.81 (d, J = 7.0 Hz, 3H), 0.79 (d, J = 6.9 Hz, 3H).

^{13}C NMR (100 MHz, DMSO- d_6): δ 171.3, 166.4, 162.9, 154.0, 146.6, 138.4, 135.7, 129.5, 128.9, 128.6, 126.8, 125.4, 123.8, 122.4, 119.4, 115.2, 114.3, 56.1, 25.3, 23.5, 22.4.

HR-MS (ESI, $[\text{M}+\text{Na}]^+$): Calcd. for $\text{C}_{28}\text{H}_{32}\text{BN}_4\text{O}_5\text{Na}$: 539.2436; Found: 539.2435

$[\alpha]_D^{20}$: -24.0 (c = 0.25, DMSO/ H_2O)

((S)-1-((R)-2-(4-((E)-(2,6-dimethylphenyl)diazenyl)benzamido)-3-phenylpropanamido)-3-methylbutyl)boronic acid (6)



74 mg (58%) of product was obtained as an orange solid. mp: 97-99 °C.

^1H NMR (400 MHz, DMSO- d_6): δ 7.96 – 7.79 (m, 4H), 7.32 – 7.13 (m, 8H), 4.67 (dd, J = 10.0, 5.1 Hz, 1H), 3.12 – 2.95 (m, 3H), 2.25 (s, 6H), 1.82 (d, J = 3.6 Hz, 1H), 1.24 – 1.10 (m, 2H), 0.83 (d, J = 7.1 Hz, 3H), 0.81 (d, J = 7.2 Hz, 3H).

^{13}C NMR (100 MHz, CDCl_3): δ 173.3, 166.8, 154.6, 150.8, 131.5, 129.5, 129.3, 128.9, 128.8, 128.3, 128.2, 127.3, 122.5, 39.8, 29.7, 25.9, 22.9, 22.5, 19.2, 17.8.

HR-MS (ESI, $[\text{M}+\text{Na}]^+$): Calcd. For $\text{C}_{29}\text{H}_{35}\text{BN}_4\text{O}_4\text{Na}$: 537.2643; Found: 537.2639

$[\alpha]_D^{20}$: -32.2 (c = 0.125, DMSO/ H_2O)

5.5 References

- (1) Siegel, R.; DeSantis, C.; Virgo, K.; Stein, K.; Mariotto, A.; Smith, T.; Cooper, D.; Gansler, T.; Lerro, C.; Fedewa, S.; Lin, C.; Leach, C.; Cannady, R. S.; Cho, H.; Scoppa, S.; Hachey, M.; Kirch, R.; Jemal, A.; Ward, E. *CA. Cancer J. Clin.* **2013**, *62*, 220.
- (2) Carelle, N.; Piotto, E.; Bellanger, A.; Germanaud, J.; Thuillier, A.; Khayat, D. *Cancer* **2002**, *95*, 155.
- (3) Szymański, W.; Beierle, J. M.; Kistemaker, H. A. V.; Velema, W. A.; Feringa, B. L. *Chem. Rev.* **2013**, *113*, 6114.
- (4) Velema, W. A.; Szymanski, W.; Feringa, B. L. *J. Am. Chem. Soc.* **2014**, *136*, 2178.
- (5) Schönberger, M.; Trauner, D. *Angew. Chemie Int. Ed.* **2014**, *53*, 3264.
- (6) Chen, X.; Wehle, S.; Kuzmanovic, N.; Merget, B.; Holzgrabe, U.; König, B.; Sotriffer, C. A.; Decker, M. *ACS Chem. Neurosci.* **2014**, *5*, 377.
- (7) Vomasta, D.; Högner, C.; Branda, N. R.; König, B. *Angew. Chem. Int. Ed. Engl.* **2008**, *47*, 7644.
- (8) Velema, W. A.; van der Berg, J. P.; Hansen, M. J.; Szymanski, W.; Driessen, A. J. M.; Feringa, B. L. *Nat. Chem.* **2013**, *5*, 924.
- (9) Mourot, A.; Fehrentz, T.; Le Feuvre, Y.; Smith, C. M.; Herold, C.; Dalkara, D.; Nagy, F.; Trauner, D.; Kramer, R. H. *Nat. Methods* **2012**, *9*, 396.
- (10) Stein, M.; Middendorp, S. J.; Carta, V.; Pejo, E.; Raines, D. E.; Forman, S. A.; Sigel, E.; Trauner, D. *Angew. Chemie Int. Ed.* **2012**, *51*, 10500.
- (11) Orlowski, R. Z.; Stinchcombe, T. E.; Mitchell, B. S.; Shea, T. C.; Baldwin, A. S.; Stahl, S.; Adams, J.; Esseltine, D.-L.; Elliott, P. J.; Pien, C. S.; Guercioli, R.; Anderson, J. K.; Depcik-Smith, N. D.; Bhagat, R.; Lehman, M. J.; Novick, S. C.; O'Connor, O. A.; Soignet, S. L. *Phase I trial of the proteasome inhibitor PS-341 in patients with refractory hematologic malignancies.*; 2002; Vol. 20, pp. 4420–4427.
- (12) Laubach, J. P.; Mahindra, A.; Mitsiades, C. S.; Schlossman, R. L.; Munshi, N. C.; Ghobrial, I. M.; Carreau, N.; Hideshima, T.; Anderson, K. C.; Richardson, P. G. The use of novel agents in the treatment of relapsed and refractory multiple myeloma. *Leukemia*, 2009, *23*, 2222–2232.
- (13) Adams, J.; Behnke, M.; Chen, S.; Cruickshank, A. A.; Dick, L. R.; Grenier, L.; Klunder, J. M.; Ma, Y. T.; Plamondon, L.; Stein, R. L. *Bioorganic Med. Chem. Lett.* **1998**, *8*, 333.
- (14) Ciechanover, A. *Angew. Chemie Int. Ed.* **2005**, *44*, 5944.
- (15) Kisselev, A. F.; Goldberg, A. L. *Chem. Biol.* **2001**, *8*, 739.
- (16) Ferrington, D. A.; Gregerson, D. S. In *Progress in Molecular Biology and Translational Science*; Tilman Grune, Ed.; The Proteasomal System in Aging and Disease; Academic Press, 2012; Vol. Volume 109, pp. 75–112.

- (17) Goldberg, A. L. *Biochem. Soc. Trans.* **2007**, 35, 12.
- (18) Ciechanover, A. *Cell* **1994**, 79, 13.
- (19) Arastu-Kapur, S.; Anderl, J. L.; Kraus, M.; Parlati, F.; Shenk, K. D.; Lee, S. J.; Muchamuel, T.; Bennett, M. K.; Driessen, C.; Ball, A. J.; Kirk, C. J. *Clin. Cancer Res.* **2011**, 17, 2734.
- (20) Richardson, P. G.; Sonneveld, P.; Schuster, M. W.; Irwin, D.; Stadtmayer, E. A.; Facon, T.; Harousseau, J.-L.; Ben-Yehuda, D.; Lonial, S.; Goldschmidt, H.; Reece, D.; San-Miguel, J. F.; Bladé, J.; Boccadoro, M.; Cavenagh, J.; Dalton, W. S.; Boral, A. L.; Esseltine, D. L.; Porter, J. B.; Schenkein, D.; Anderson, K. C. *N. Engl. J. Med.* **2005**, 352, 2487.
- (21) Park, S. B.; Goldstein, D.; Krishnan, A. V; Lin, C. S.-Y.; Friedlander, M. L.; Cassidy, J.; Koltzenburg, M.; Kiernan, M. C. *CA. Cancer J. Clin.* **2013**, 63, 419.
- (22) Kisselev, A. F.; van der Linden, W. A.; Overkleeft, H. S. *Chem. Biol.* **2012**, 19, 99.
- (23) Adams, J.; Palombella, V. J.; Sausville, E. A.; Johnson, J.; Destree, A.; Lazarus, D. D.; Maas, J.; Pien, C. S.; Prakash, S.; Elliott, P. J. *Cancer Res.* **1999**, 59, 2615.
- (24) Groll, M.; Ditzel, L.; Löwe, J.; Stock, D.; Bochtler, M.; Bartunik, H. D.; Huber, R. *Nature* **1997**, 386, 463.
- (25) Groll, M.; Berkers, C. R.; Ploegh, H. L.; Ovaa, H. *Structure* **2006**, 14, 451.
- (26) Zhu, Y.; Zhao, X.; Zhu, X.; Wu, G.; Li, Y.; Ma, Y.; Yuan, Y.; Yang, J.; Hu, Y.; Ai, L.; Gao, Q. *J. Med. Chem.* **2009**, 52, 4192.
- (27) Hamon, F.; Djedaini-Pilard, F.; Barbot, F.; Len, C. *Tetrahedron* **2009**, 65, 10105.
- (28) Briquet, L.; Vercauteren, D. P.; Perpète, E. A.; Jacquemin, D. *Chem. Phys. Lett.* **2006**, 417, 190.
- (29) Briquet, L.; Vercauteren, D. P.; André, J.-M.; Perpète, E. A.; Jacquemin, D. *Chem. Phys. Lett.* **2007**, 435, 257.
- (30) Beharry, A. A.; Woolley, G. A. *Chem. Soc. Rev.* **2011**, 40, 4422.
- (31) Szymanski, W.; Beierle, J. M.; Kistemaker, H. A. V; Velema, W. A.; Feringa, B. L. *Chem. Rev.* **2013**, 113, 6114.
- (32) Göstl, R.; Senf, A.; Hecht, S. *Chem. Soc. Rev.* **2014**, 43, 1982.
- (33) Bandara, H. M. D.; Burdette, S. C. *Chem. Soc. Rev.* **2012**, 41, 1809.
- (34) Mendonça, C. R.; Balogh, D. T.; De Boni, L.; dos Santos, D. S.; Zucolotto, V.; Oliveira, O. N. *Molecular Switches*; Feringa, B. L.; Browne, W. R., Eds.; 2nd ed.; 2011.
- (35) Zbaida, S. *Drug Metab. Rev.* **1995**, 27, 497.
- (36) Boulègue, C.; Löweneck, M.; Renner, C.; Moroder, L. *Chembiochem* **2007**, 8, 591.

- (37) Lopez-Mirabal, H. R.; Winther, J. R. Redox characteristics of the eukaryotic cytosol. *Biochimica et Biophysica Acta - Molecular Cell Research*, 2008, 1783, 629–640.
- (38) Renner, C.; Moroder, L. *Chembiochem a Eur. J. Chem. Biol.* **2006**, 7, 868.
- (39) Samanta, S.; Beharry, A. a; Sadovski, O.; McCormick, T. M.; Babalhavaeji, A.; Tropepe, V.; Woolley, G. A. *J. Am. Chem. Soc.* **2013**, 135, 9777.
- (40) Beharry, A. A.; Wong, L.; Tropepe, V.; Woolley, G. A. *Angew. Chem. Int. Ed. Engl.* **2011**, 50, 1325.
- (41) Szymański, W.; Wu, B.; Poloni, C.; Janssen, D. B.; Feringa, B. L. *Angew. Chemie Int. Ed.* **2013**, 52, 2068.
- (42) Ovaa, H.; van Swieten, P. F.; Kessler, B. M.; Leeuwenburgh, M. A.; Fiebiger, E.; van den Nieuwendijk, A. M. C. H.; Galardy, P. J.; van der Marel, G. A.; Ploegh, H. L.; Overkleeft, H. S. *Angew. Chemie Int. Ed.* **2003**, 42, 3626.
- (43) Verdoes, M.; Florea, B. I.; Menendez-Benito, V.; Maynard, C. J.; Witte, M. D.; van der Linden, W. A.; van den Nieuwendijk, A. M. C. H.; Hofmann, T.; Berkers, C. R.; Van Leeuwen, F. W. B.; Groothuis, T. A.; Leeuwenburgh, M. A.; Ovaa, H.; Neefjes, J. J.; Filippov, D. V.; van der Marel, G. A.; Dantuma, N. P.; Overkleeft, H. S. *Chem. Biol.* **2006**, 13, 1217.
- (44) Li, N.; Kuo, C.-L.; Paniagua, G.; van den Elst, H.; Verdoes, M.; Willems, L. I.; van der Linden, W. a; Ruben, M.; van Genderen, E.; Gubbens, J.; van Wezel, G. P.; Overkleeft, H. S.; Florea, B. I. *Nat. Protoc.* **2013**, 8, 1155.
- (45) Mosmann, T. *J. Immunol. Methods* **1983**, 65, 55.
- (46) Frazier, C. C. *Int. J. Dermatol.* **1996**, 35, 312.
- (47) Kalka, K.; Merk, H.; Mukhtar, H. *J. Am. Acad. Dermatol.* **2000**, 42, 389.
- (48) Bléger, D.; Schwarz, J.; Brouwer, A. M.; Hecht, S. *J. Am. Chem. Soc.* **2012**, 134, 20597.
- (49) Molander, G. A.; Cavalcanti, L. N. *J. Org. Chem.* **2012**, 77, 4402.
- (50) Lim, Y.-K.; Lee, K.-S.; Cho, C.-G. *Org. Lett.* **2003**, 5, 979.
- (51) Nishioka, H.; Liang, X.; Kashida, H.; Asanuma, H. *Chem. Commun. (Camb).* **2007**, 4354.
- (52) Kreger, K.; Wolfer, P.; Audorff, H.; Kador, L.; Stingelin-Stutzmann, N.; Smith, P.; Schmidt, H.-W. *J. Am. Chem. Soc.* **2010**, 132, 509.
- (53) Inglis, S. R.; Woon, E. C. Y.; Thompson, A. L.; Schofield, C. J. *J. Org. Chem.* **2010**, 75, 468.
- (54) Dorsey, B. D.; Iqbal, M.; Chatterjee, S.; Menta, E.; Bernardini, R.; Bernareggi, A.; Cassarà, P. G.; D'Arasmo, G.; Ferretti, E.; De Munari, S.; Oliva, A.; Pezzoni, G.; Allievi, C.; Strepponi, I.; Ruggeri, B.; Ator, M. A.; Williams, M.; Mallamo, J. P. *J. Med. Chem.* **2008**, 51, 1068.

